RSC Advances

This article can be cited before page numbers have been issued, to do this please use: A. Samanta, S. Jana, R. K. Das and Y. Chang, *RSC Adv.*, 2014, DOI: 10.1039/C3RA46208K.

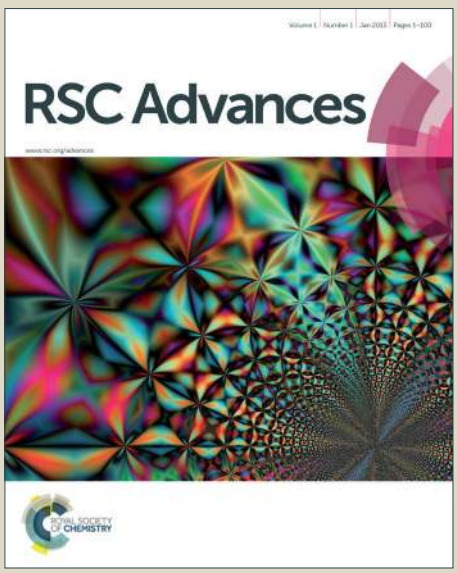

ROYAL SOCIETY OF CHEMISTRY

www.rsc.org/advances

View Article Online
DOI: 10.1039/C3RA46208K

Wavelength and shape dependent SERS study to develop ultrasensitive nanotags for imaging of cancer cells

Animesh Samanta,[!,a] Santanu Jana,[!,a] Raj Kumar Das [b] and Young-Tae Chang* [a,b]

[a]Laboratory of Bioimaging Probe Development, Singapore Bioimaging Consortium, Agency for Science, Technology and Research (A*STAR), Singapore

[b]Department of Chemistry, National University of Singapore, 3 Science Drive 3, 117543, Singapore.

[!] Authors have equal contribution

E-mail: chmcyt@nus.edu.sg

Abstract: The Raman signal enhancement depends on mainly four critical factors. These factors are localized surface plasmon resonance (LSPR) of gold substrates along with shape and electronic absorbance of Raman reporters along with laser sources. Hence, the effect of these all four parameters were systematically studied by changing either the different geometries/shapes of gold substrates having a wide range of SPR or electronic absorbance of Raman reporters under a fixed laser excitation of 633 nm or 785 nm. Enhancement factor (EF) values were evaluated for individual substrate with respect to five different Raman reporters which cover the maximum absorbance from 530 nm to 800 nm. The EF values suggest that more than minimum ten times signal intensity has been increased compare to previous report. Among five different shape of gold nanoparticles, gold nanostar (GNSt) is happened to be most suitable substrate for the highest signal enhancement under both excitation laser sources. Gold nanosphere (GNSp) is the second best at 633 nm laser excitation; however it is the modest substrate for SERS enhancement at 785 nm laser excitation. After finding the key tools for the development of ultrasensitive SERS nanoprobes, we selected best Raman reporter (Cy7LA) for the development of biocompatible SERS nanotags in three different SERS substrates for the effective detection of cancer cells under 785 nm laser source.

Introduction

Surface-enhanced Raman spectroscopy (SERS) is a valuable analytical tool for the ultrasensitive identification and quantification of host of molecules ranging from chemical warfare agents, dyestuffs to biomolecules [1-3]. Despite the substantial success of fluorescence

View Article Online
DOI: 10.1039/C3RA46208K

based bio-imaging, the technique is often limited by the sensitivity, photostability and cytotoxicity [4-6]. In SERS technique, using the inelastic light scattering of nobel metal nanoparticles paves the way of application era of Raman spectroscopy due to its potentiality in overcoming the low sensitivity problem which is quite inherent in conventional Raman spectroscopy [7-8]. Therefore, SERS techniques which provide a unique spectral fingerprint of a single molecule with high sensitivity have facilitated to overcome two major concerns in the field of bio-imaging such as sensitivity and biocompatibility. Among the most common SERS substrates (Au, Ag, Cu), gold nanoparticles have been considered as the most suitable substrate for ultrasensitive bio-imaging platform due to their non-cytotoxicity, water solubility, long-term stability and good biocompatibility [9-12]. Notable aspects of the SERS technique such as fruitfulness of spectroscopic information and high sensitivity towards bio-analytes, have motivated many researchers which are associated with the design of different shape and sizes of gold substrates. Optically tuned SERS substrates involving nanorods, hollow nanostructures, nanostars and nanoflowers have been developed to create NIR-active hot spots to gain the high sensitivity [13-18]. Alternatively, 60 nm diameter of nanospheres have been used to develop ultrasensitive NIR nanoprobes for the detection of tumor by applying NIR active Raman reporters which can resonance with NIR excitation laser source such as diode laser, 785 nm; to generate surface enhanced resonance Raman scattering (SERRS) [19]. Therefore, shape and surface plasmon resonance (SPR) of colloidal gold nanoparticles play a major role to enhance the sensitivity of Raman scattering when it undergoes resonance with specific wavelength of Raman reporters under specific excitation laser source. To date, a systematic study has been carried out on different sizes of the spherical nanoparticles, and found that 40- 60 nm nanoparticles are preferable for obtaining the highest signal intensity [20-22]. However, there is no systematic study to investigate the influence of the combination effects of both shapes and SPR of gold substrates with absorbance wavelengths of Raman

View Article Online
DOI: 10.1039/C3RA46208K

reporters and under certain laser excitation source. Recently, Li et al. reported shape dependent (sphere, rod and star) SERS study to compare their relative intensity [23]. However, their study was based on 15 nm gold nanosphere which is known to be very poor gold substrates in view of the SERS intensity. Furthermore, their study was only focused on a single Raman reporter (MGITC) which was not suitable for SERRS study. Therefore, a systematic study on four major parameters such as a) shape of the substrates, b) SPR of substrates, c) electronic absorbance of Raman reporters and finally d) excitation wavelength of laser sources may open a new window for the development of ultrasensitive nanoprobes. Herein, we report a systematic SERRS study using five gold substrates with different shapes along with variable LSPR and five different Raman reporters with variable absorptions wavelengths to find out the most suitable combinations for the development of ultrasensitive SERS nanotags. Furthermore, the most suitable Raman reporter has been applied to prepare ultrasensitive nanotgas by varying three different geometries such as gold nanosphere (GNSp), gold nanorod-800 (GNR-800), and gold nanostar (GNSt). These three different nanotags have been applied for the detection of oral squamous cell carcinoma cells.

Result and Discussion

Design

In this study, we have selected five cyanine dyes with diverse absorbance-wavelengths ranging from visible to near infrared (NIR) region. It is well studied that cyanine dyes are good Raman active organic dyes [24-26]. Our research group previously demonstrated that the incorporation of lipoic acid (LA) to the cyanine dyes was the key strategy for making suitable Raman reporters in the process of chemisorption on the surface of gold substrates [27]. In this regard, we have chosen Cy3LA, Cy5LA, Cy7LA, Cy7.5LA and CyNAMLA-381 as Raman reporters [8, 19, 27-28]. The structures of five different Raman reporters are shown in Fig.

View Article Online
DOI: 10.1039/C3RA46208K

1a in which the alternative vinylene functional groups play key role for the absorbance of light from Vis-NIR regions. The maximum electronic absorbance of cyanine based Raman reporters are 540 nm, 645 nm, 750 nm, 740-790 nm, and 790 nm for Cy3LA, Cy5LA, Cy7LA, Cy7.5LA and CyNAMLA-381 respectively (Fig 1b; Fig. S1). These Raman reporters are considered to be appropriate choice for systematic study of wavelength dependent SERS signal's enhancement.

Furthermore, we also have chosen five different gold substrates; GNSp, GNR-700, GNR-800, GNR-900 and GNSt which display wide range of surface plasmon resonance (SPR) to understand the effects of wavelength and geometry on Raman enhancement. Fig. 1c displays a UV-Visible-NIR surface plasmon resonance among different gold substrates and their corresponding TEM images in Fig. 1d are shown in their different geometries such as sphere, star and three different rods. According to the SPR, the GNSp shows maximum around 535 nm, and three different gold GNRs show at maximum 700 nm, 800 nm and 900 nm depending on the length of the nanorod, whereas the GNSt covers the broad range from 500-900 nm. Eventually, the EF values of Raman reporters exhibit variable effects depending on the SPR value in identical condition of two different laser excitations (i.e. 633 nm and 785 nm).

Synthesis

Herein, we used 60 nm GNSp, and three different GNRs such as GNR-700, GNR-800 and GNR-900 and GNSt were prepared according to the well-documented seed-mediated growth methods [29-35]. Five different Raman reporters were synthesized according to our previously reported methods [19, 27, 28].

View Article Online
DOI: 10.1039/C3RA46208K

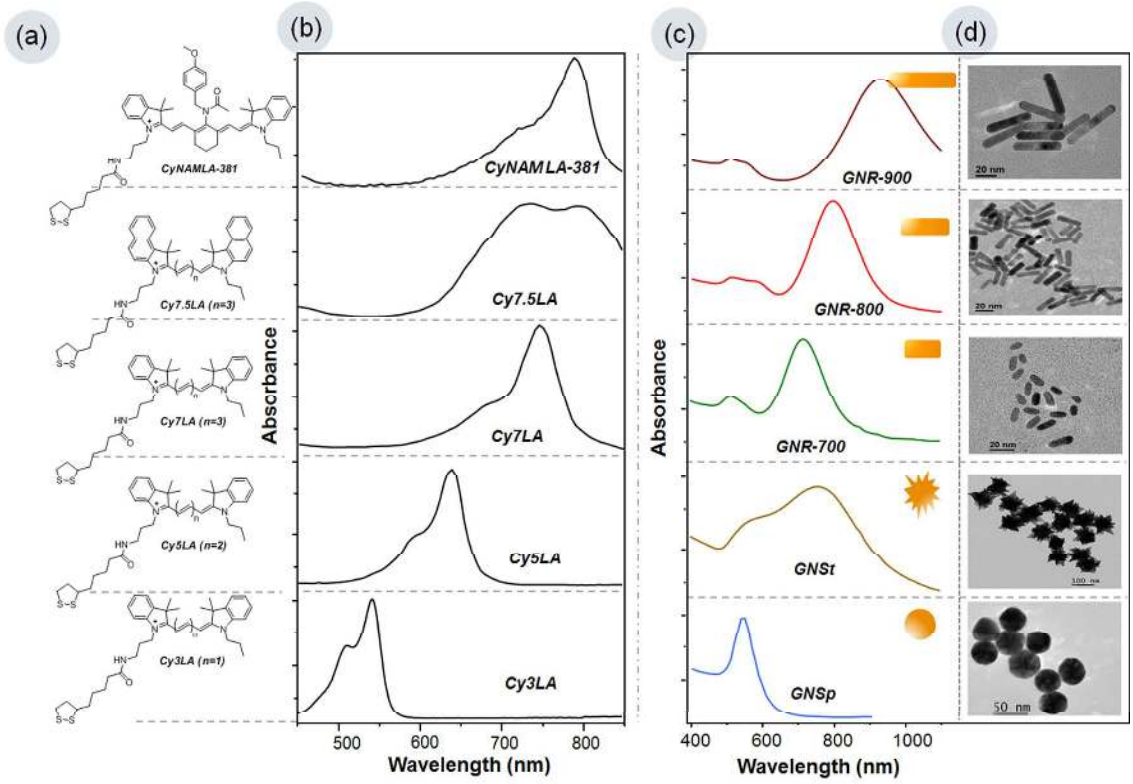

Fig 1. (a) & (b) Structure of Cy3LA. Cy5LA, Cy7LA, Cy7.5LA, CyNAMLA-381 and their corresponding Vis-NIR absorbance spectra in aqueous solution (540 nm, 645 nm, 750 nm, 740-790 nm and 790 nm). (c) SPR of GNSp, GNSt, GNR-700, GNR-800 and GNR900 and their corresponding d) TEM images.

Enhancement Factor (EF)

Applying different combinations of gold substrates and Raman reporters, we measured the EF under visible and NIR laser excitation wavelengths. Here, we fixed the concentrations of Raman reporters and then varied the concentrations of gold substrates in order to reach the saturation point. As different shapes of gold substrates are stabilized with different surfactants, sodium citrate stabilized GNSp, and polyvinylpyrrolidone (PVP) coated GNSt were incubated for 10 min for the replacement by lipoic acid of Raman reporters. However, CTAB stabilized GNRs was incubated for overnight. The spectra were recorded after complete adsorption of the dyes on nanoparticles. The maximum SERS enhancement was found at concentration of all the gold substrates as follows: 6.5 nM for GNSp, 1.8 nM for GNRs and 6 nM for GNSt (Fig. S3). At this saturation point, we calculated the enhancement

View Article Online
DOI: 10.1039/C3RA46208K

factor (EF) of five different Raman reporters with each gold substrate. Thus, the calculated EF values provide a clear picture to investigate the relation between the different parameters and signal enhancement effect. The EF was calculated according to the following equation (1) [23, 36-37] in which the maximum peak intensity of each signature molecule was considered at 552, 555, 503, 586, and 523 cm^{-1} for Cy3LA, Cy5LA, Cy7LA, Cy7.5L and CyNAMLA-381 respectively (Fig. S2).

$$EF = \frac{I_{SERS}}{I_b} \frac{C_b}{C_{SERS}} \qquad (1)$$

In this equation (1), I_{SERS} and C_{SERS} are the Raman intensities and the molar concentrations of our signature molecules (Cy3LA, Cy5LA, Cy7LA, Cy7.5LA and CyNAMLA-381) in the presence of gold nanoparticles. Similarly, I_b and C_b are the Raman intensities and the molar concentrations of signature molecules in the absence of gold nanoparticles.

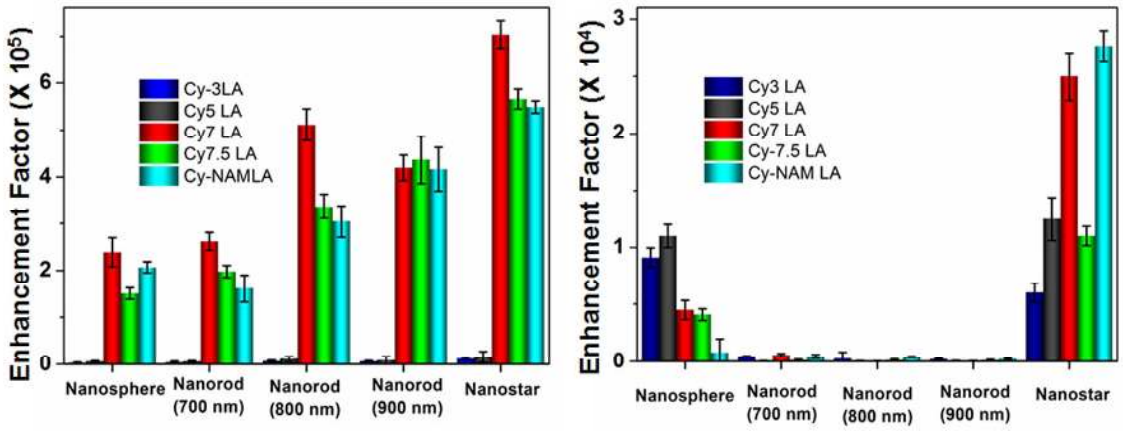

Figure 2. (a) Relative SERS intensity among different geometry of gold substrates under the excitation laser source at 785 nm (b) under the excitation laser source at 633 nm. Five different Raman reporters contribute for the enhancement of Raman intensity by resonance of their electronic absorbance with substrates SPR and laser.

Table 1. EF value calculation of five different Raman reporters with respect to five different gold substrates under 785 nm and 633 nm laser excitation wavelengths.

View Article Online
DOI: 10.1039/C3RA46208K

		Dye									
		Cy-3 LA		Cy-5 LA		Cy-7 LA		Cy-7.5 LA		CyNAMLA 381	
		633 nm ($\times 10^4$)	785 nm ($\times 10^5$)	633 nm ($\times 10^4$)	785 nm ($\times 10^5$)	633 nm ($\times 10^4$)	785 nm ($\times 10^5$	633 nm ($\times 10^4$)	785 nm ($\times 10^5$)	633 nm ($\times 10^4$)	785 nm ($\times 10^5$)
Au nanostructure (surface Plasmon)	Sphere (540 nm)	0.91	0.15	0.88	0.18	0.46	2.6	0.41	1.5	0.08	2.1
	Nanorod (700 nm)	0.06	0.19	0.008	0.23	0.05	2.8	0.02	1.9	0.015	1.8
	Nanorod (800 nm)	0.02	0.23	0.005	0.20	0.006	5.2	0.01	3.2	0.02	3.1
	Nanorod (900 nm)	0.03	0.21	0.002	0.18	0.005	4.1	0.015	4.2	0.003	4.2
	Nano Star (600-900 nm)	0.59	0.33	1.21	0.23	2.46	6.9	1.06	5.8	2.71	5.7

Table 1 and Fig 2 clearly indicate that EF values are in order of 10^5 orders whenever we excited at 785 nm laser excitation and 10^4 orders at 633 nm excitation. We have seen that the trend of relative Raman signal enhancement among different shapes is similar to previous report i.e. nanostar > nanorods > nanosphere. However, the EF values are ten times higher than earlier report. This high EF values were achieved in this experiments due to the combine effects of resonance with excitation laser source and the electronic absorbance of Raman reporters along with SPR of gold substrates. Furthermore, different shapes contribute their inherent alignment to generate maximum electric field intensity and generation of "hot spots". Henceforth, we discussed the effects of each parameter with more details.

Effects of absorbance of Raman reporters on EF

Table 1 results suggest that the electronic absorbance of reporters play important roles for signal enhancement. Visible light absorbing Cy3LA and Cy5LA showed least enhancement compare to NIR light absorbing Cy7LA, Cy7.5LA and CyNAMLA-381 (Fig. 2), under the 785 laser source. This is due to the resonance between electronic absorbance of NIR Raman reporters and NIR laser source. Interestingly, we found that Cy7LA showed the highest EF compared to other NIR light absorbing reporter molecules. Here, the possible reason could be

View Article Online
DOI: 10.1039/C3RA46208K

attributed to the minimum energy dissipation via fluorescence incidence. However, the other two NIR signature molecules (Cy7.5LA and CyNAMLA-381) lose partial energy through its emission while application of excitation laser source at 785 nm.

Effects on EF of surface plasmons resonance of gold substrates

SPR of gold substrates show also effective roles for signal enhancement along with the absorbance of reporters. Among three different gold nanorods, enhancement effect-wise, GNR-700 display much weaker consequence than its other counterpart (GNR-800 and GNR-900) due to the very less resonance efficiency with 785 nm laser. Here, GNR-800 is expected to be shown better signal due to its perfect in overlap with 785 nm excitation laser source however, we observed that GNR-900 even little better than GNR-800. This can be explained in a way that GNR-900 was dominating its inherent alignment to generate maximum electric field intensity rather than the resonance with the excitation laser source. Additional weaker SPR bands of GNRs, appeared around 530 nm wavelengths can partially contribute to resonance with the 633 nm excitation lasers. Among three nanorods, GNR-700 showed little better than other two as they almost do not have any surface plasmon at 633 nm (Fig. 2). Furthermore, GNSt showed the highest EF values compare to GNRs or GNSp in both excitation laser source at 785 nm or 633 nm. This phenomenon is attributed due to the broad localized SPR of nanostars ranging from 500 nm to 900 nm along with its characteristic shape.

Effects of shapes of gold substrates

The special shape of nanostars plays most vital role to generate the maximum electric field intensity which causes the highest signal intensity in both laser excitations. Maximum electromagnetic field intensity which was intensified at the sharp tips of nanostars developed SPR at NIR regions around 700-800 nm, [23, 38-40]. This defined localized SPR of GNSt can generate “hot spots” around the sharp tips, resulting to obtain highly sensitive SERS signals

View Article Online
DOI: 10.1039/C3RA46208K

under 785 nm laser source. Furthermore, an another shoulder band which is due to the surface plasmon resonance (SPR) of sphere like central core structure of GNSt contributes to enhance Raman scattering at 633 nm laser excitation. In contrary, maximum electromagnetic field which was concentrated at two longitudinal ends of GNRs, qualify the highest SERS intensity after the resonance with 785 nm laser [41-43]. Interestingly, the result indicates that the longitudinal ends of nanorods are aligned towards parallel to NIR laser excitation, caused the most significant SERS enhancement. However, GNSp lacks the advantages which are present in GNRs or GNSt. Therefore, it has least structural effects to induce the SERS enhancement in identical experimental conditions. After considering the effects of different parameters on SERS, we conclude that the most sensitive NIR Raman reporter is Cy7LA among others and nanostar was the most suitable substrate for the generation of NIR "hot spots" to develop an NIR ultrasensitive nanoparobes. Therefore, this Cy7LA was further applied for cancer cells imaging by changing the different substrates from sphere, star to rods.

Cytotoxicity: Gold nanoparticles are known to be least toxic metal nanoparticles compared to silver and other heavy metals. Therefore, an extensive research studies have been focused for the development of nanoprobes based on gold nanoparticles. We have previously demonstrated the suitability of the nanoprobes for *in vivo* imaging and kinetics study for 8 days to demonstrate the biocompatibility [28]. In this study, we performed cytotoxicity assay in OSCC cell line to validate the biocompatibility of these SERS nanotags *in vitro* system. We have considered few representative combinations to test the cell viability by applying CCK-8 assay. We represent here two dyes (Cy-7LA and Cy7.5LA) with varies concentration (4 & 2 μM) and three different set of nanotags such as GNSp@Cy-7LA@PEG, GNSt@Cy-7LA@PEG, GNR@Cy-7LA@PAA and GNSp@Cy-7.5LA@PEG. Interestingly, we found the Au-conjugates and even the dye alone didn't show high cytotoxicity; the cells almost >90% viable with respect to control (Fig. 3).

View Article Online
DOI: 10.1039/C3RA46208K

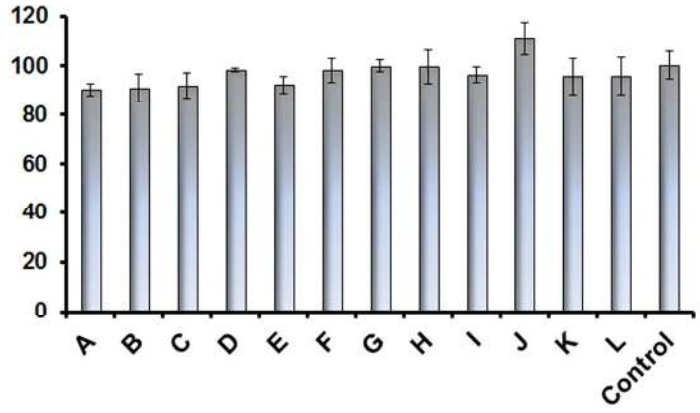

Figure 3. Cell viability of OSCC cells after 3 h incubation with A. GNSp@Cy-7.5LA@PEG (5.66 x 10^{-8} M); B. GNSp@Cy-7.5LA@PEG (2.88 x 10^{-8} M); C. Cy-7LA (4 x 10^{-6} M); D. Cy-7LA (2 x 10^{-6} M); E. GNSp@Cy7LA@PEG (5.66 x 10^{-8} M); F. GNSp@Cy-7LA@PEG (2.88 x 10^{-8} M); G. GNSt@Cy7LA@PEG (2.5 x 10^{-8} M); H. GNSt@Cy-7LA@PEG(1.25 x 10^{-8} M); I. Cy-7.5LA (4 x 10^{-6} M); J. Cy-7.5LA (2 x 10^{-6} M); K. GNR@Cy-7LA@PAA (2.5 x 10^{-8} M); L. GNR@Cy-7LA@PAA(1.25 x 10^{-8} M); Control: PBS buffer without any dye or gold nanoparticles.

Cancer cells Imaging

Now, using the most suitable Raman reporter (Cy7LA), we prepared three different nanotags named as Cy7LA@GNSp@PEG-anti-EGFR, Cy7LA@GNR-800@PAA-anti-EGFR and Cy7LA@GNSt@PEG-anti-EGFR for inspecting target specific recognition in live cancer cells. For the preparation of biocompatible SERS nanotags, mixed PEG or poly acrylic acid (PAA) ligands were encapsulated to the gold substrates which were already saturated by Cy7LA reporter. It should be noted that PAA, an encapsulating agent was applied to nanorods instead of PEG which was not effective to replace the CTAB even after 24 h incubations. After encapsulation of PEG or PAA to the nanoparticles, these were characterized by TEM images. There was no aggregation among the particles (Fig. S5). Next, these stable biocompatible nanotags were conjugated with specific targeted antibody i.e. anti-EGFR for targeting epidermal growth factor receptors (EGFR), an over expressed receptors on the cell membrane in oral squamous cell carcinoma (OSCC) cells [4, 10, 44-46]. After successful conjugation of antibody through amide coupling, these nanotags were

View Article Online
DOI: 10.1039/C3RA46208K

characterized by means of measurement of SERS intensity as well as absorbance spectra of proteins at 280 nm (Fig.S4). Finally, we incubated antibody modified SERS nanotags to the cells and scanned at 503 cm^{-1} and 554 cm^{-1} to get clear images of specific cancer cells from the cell surface receptors (Fig. 4). Contrary, anti-HER2 conjugated nanoparticles does not show any significant SERS signal from cell surfaces (Fig. S6).

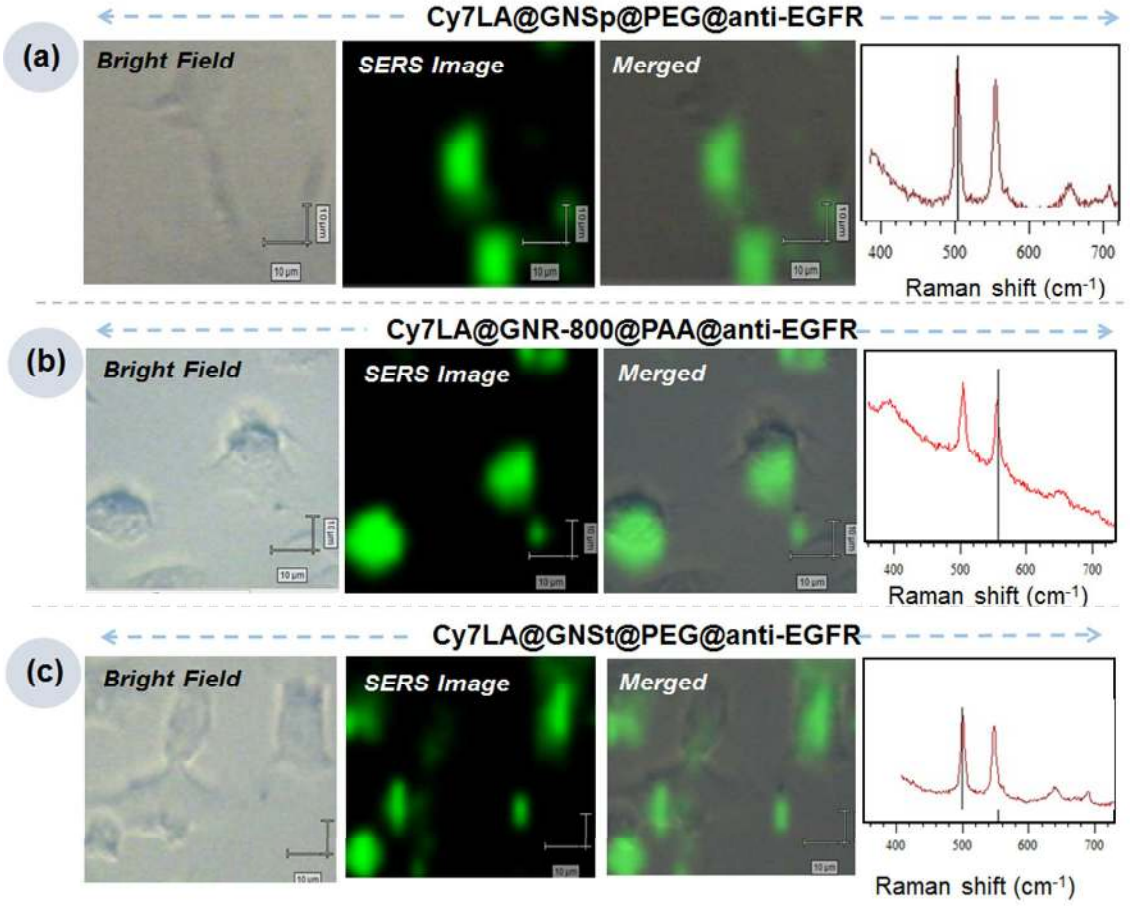

Figure 4. a) OSCC cell images by SERS nanotags (Cy7LA@GNSp@PEG-anti-EGFR): in a row BF image of OSCC cells; SERS image at 503 cm^{-1} and merged images. b) OSCC cell images by SERS nanotags (Cy7LA@GNR-800@PAA-anti-EGFR: in a row BF image of OSCC cells; SERS image at 554 cm^{-1} and merged images. c) OSCC cell images by SERS nanotags (Cy7LA@GNSt@PEG-anti-EGFR: in a row BF image of OSCC cells; SERS image at 503 cm^{-1} and merged images.

We successfully demonstrated the specific recognition of OSCC cells by using three individual nanotags. Eventually, cell mapping experiment clearly confirms that these

View Article Online
DOI: 10.1039/C3RA46208K

nanotags are capable of specific recognitions of cell surface receptors on the cell membranes. Moreover, these cell mapping images are well correlated with the previously reported results [47]. These experiments were performed by using minimum amount of nanotags (final concentration of nanotags: 10 μL x 400 pM diluted to 500 μL final volume: i.e 8 pM). The concentrations used here, was much low compared to previous report [8]. In this research study, we focused mainly on the application of effective cancer cell imaging using these nanotags.

Conclusions

We reported a systematic study on the influence of SERS signal enhancement based on the variance of four most effective parameters that play major role for enhancing SERS signals. Here, we successfully demonstrated that the selection of four major parameters such as geometry of gold substrates, LSPR of gold substrates, electronic absorption wavelengths of Raman reporters and laser sources are the key component for the development of ultrasensitive SERS nanotags. From the study, it is obvious that the SERS signal enhancement was strongly depend on the wavelength of the Raman reporters and LSPR of gold substrates along with geometry of the substrates. The most suitable combination, we found for the development of an ultrasensitive NIR SERS probe is nanostar as a gold substrate along with Cy7LA as Raman reporter. The second and third most suitable conditions are GNR-900 and GNR-800 along with Cy7LA. The last, suitable NIR SERS nanoprobes can be prepared by the combination of 60 nm GNSp along with Cy7LA. Nanostar substrates can be used as most suitable candidate for visible SERS probe development. Nanosphere is much better than nanorods while choosing Raman reporters as visible light absorbing candidates. These new finding with systematic study may routinely help in future for developing ultrasensitive SERS nanoprobes. For the proof of concept, we

View Article Online
DOI: 10.1039/C3RA46208K

have presented here a cancer cell imaging application by using these new biocompatible SERS probes.

Acknowledgements

We gratefully acknowledge the A*STAR Joint Council Office (JCO), Singapore (Grant 1231AFG028) for the financial support.

References

1) M. Leona, J. Stenger and E. Ferloni, *J. Raman. Spectrosc.*, **2006**, *37*, 981-992.
2) (a) Y. S. Huh, A. J. Chung, B. Cordovez and D. Erickson, *Lab. Chip.*, **2009**, *9*, 433-439. (b) K. Kneipp, H. Kneipp, I. Itzkan, R. R. Dasari and M. S. Feld, *J. Phys. Condens. Mat.*, **2002**, *14*, R597-R624.
3) C. David, N. Guillot, H. Shen, T. Toury and M. L. de la Chapelle, *Nanotechnology*, **2010**, *21*, 475501–475501.
4) X. M. Qian, X. H. Peng, D. O. Ansari, Q. Yin-Goen, G. Z. Chen, D. M. Shin, L. Yang, A. N. Young, M. D. Wang and S. M. Nie, *Nat. Biotechnol.,* **2008**, *26*, 83-90.
5) S. Kim, Y. T. Lim, E. G. Soltesz, A. M. De Grand, J. Lee, A. Nakayama, J. A. Parker, T. Mihaljevic, R. G. Laurence, D. M. Dor, L. H. Cohn, M. G. Bawendi and J. V. Frangioni, *Nat. Biotechnol.,* **2004**, *22*, 93-97.
6) M. N. Rhyner, A. M. Smith, X. Gao, H. Mao, L. Yang and S. Nie, *Nanomedicine,* **2006**, *1*, 209-217.
7) W. J. Cho, Y. Kim and J. K. Kim, *ACS Nano* **2012**, *6*, 249-255.
8) K. K. Maiti, A. Samanta, M. Vendrell, K. S. Soh, M. Olivo and Y. T. Chang, *Chem. Commun.* **2011**, *47*, 3514-3516.
9) K. K. Maiti, U. S. Dinish, C. Y. Fu, J. J. Lee, K. S. Soh, S. W. Yun, R. Bhuvaneswari, M. Olivo and Y. T. Chang, *Biosens. Bioelectron.* **2010**, *26*, 398-403.
10) S. Lee, H. Chon, S. Y. Yoon, E. K. Lee, S. I. Chang, D. W. Lim, J. Choo, *Nanoscale*, **2012**, *4*, 124-129.
11) B. Sharma, R. R. Frontiera, A. I. Henry, E. Ringe and R. P. Van Duyne, *Materials Today,* **2012**, *15*, 16-25.
12) T. Vo-Dinh, F. Yan and M. B. Wabuyele, *J. Raman. Spectrosc.*, **2005**, *36*, 640-647.

View Article Online
DOI: 10.1039/C3RA46208K

13) K. D. Alexander, K. Skinner, S. P. Zhang, H. Wei and R. Lopez, *Nano Lett.*, **2010**, *10*, 4488-4493.

14) B. Nikoobakht and M. A. El-Sayed, *J. Phys. Chem. A.*, **2003**, *107*, 3372-3378.

15) C. Hrelescu, T. K. Sau, A. L. Rogach, F. Jäckel, G. Laurent, L. Douillard, F. Charra. *Nano Lett.,* **2011**, *9,* 402-407.

16) D. Xu, J. J. Gu, W. N. Wang, X. C. Yu, K. Xi and X. D. Jia, *Nanotechnology,* **2010**, *21*.

17) Q. Li, Y. Y. Jiang, R. C. Han, X. L. Zhong, S. Y. Liu, Z. Y. Li, Y. L. Sha and D. S. Xu, *Small*, **2013**, *9*, 927-932.

18) C. G. Khoury and T. Vo-Dinh, *J. Phys. Chem. C*, **2008**, *112*, 18849-18859.

19) A. Samanta, K. K. Maiti, K. S. Soh, X. J. Liao, M. Vendrell, U. S. Dinish, S. W. Yun, R. Bhuvaneswari, H. Kim, S. Rautela, J. H. Chung, M. Olivo and Y. T. Chang, *Angew. Chem. Int. Edit.*, **2011**, *50*, 6089-6092.

20) N. Nath and A. Chilkoti, *Anal. Chem.*, **2004**, *76*, 5370-5378.

21) V. Joseph, A. Matschulat, J. Polte, S. Rolf, F. Emmerling and J. Kneipp, *J. Raman. Spectrosc.*, **2011**, *42*, 1736-1742.

22) S. Link, and M. A. El-Sayed, *J. Phys. Chem. B.,* **1999**, *103***,** 4212-4217.

23) M. Li, S. K. Cushing, J. Zhang, J. Lankford, Z. P. Aguilar, D. Ma and N. Wu, *Nanotechnology,* **2012**, *23*, 115501.

24) W. Leng and A. M. Kelley, *J. Am. Chem. Soc.,* **2006**, *128*, 3492-3493.

25) K. K. Maiti, A. Samanta, M. Vendrell, K. S. Soh, M. Olivo and Y. T. Chang, *Chem. Commun.,* **2011**, *47*, 3514-3516.

26) G. von Maltzahn, A. Centrone, J. H. Park, R. Ramanathan, M. J. Sailor, T. A. Hatton and S. N. Bhatia, *Adv. Mater.*, 2009, **21**, 3175-3180.

27) K. K. Maiti, U. S. Dinish, C. Y. Fu, J. J. Lee, K. S. Soh, S. W. Yun, R. Bhuvaneswari, M. Olivo and Y. T. Chang, *Biosens. Bioelectron.,* **2010**, *26*, 398-403.

28) K. K. Maiti, U. S. Dinish, A. Samanta, M. Vendrell, K. S. Soh, S. J. Park, M. Olivo and Y. T. Chang, *Nano Today,* **2012**, *7*, 85-93.

29) X. C. Ye, L. H. Jin, H. Caglayan, J. Chen, G. Z. Xing, C. Zheng, D. N. Vicky, Y. J. Kang, N. Engheta, C. R. Kagan and C. B. Murray, *ACS Nano,* **2012**, *6*, 2804-2817.

30) P. S. Kumar, I. Pastoriza-Santos, B. Rodriguez-Gonzalez, F. J. Garcia de Abajo and L. M. Liz-Marzan, *Nanotechnology,* **2008**, *19,*15606.

31) M. Schutz, D. Steinigeweg, M. Salehi, K. Kompe and S. Schlucker, *Chem. Commun.,* **2011**, *47*, 4216-4218.

View Article Online
DOI: 10.1039/C3RA46208K

32) M. Yamamoto, Y. Kashiwagi, T. Sakata, H. Mori and M. Nakamoto, *Chem. Mater.*, **2005**, *17*, 5391-5393.

33) S. E. Lohse and C. J. Murphy, *Chem. Mater.*, **2013**, *25*, 1250-1261.

34) A. M. Gabudean, D. Biro and S. Astilean, *Nanotechnology*, **2012**, *23*, 485706.

35) N. R. Jana, L. Gearheart and C. J. Murphy, *J. Phys. Chem. B*, **2001**, *105*, 4065-4067.

36) E. C. Le Ru, E. Blackie, M. Meyer and P. G. Etchegoin, *J. Phys. Chem. C*, **2007**, *111*, 13794-13803.

37) P. H. C. Camargo, C. M. Cobley, M. Rycenga and Y. N. Xia, *Nanotechnology*, **2009**, *20,* 434020.

38) C. G. Khoury and T. Vo-Dinh, *J. Phys. Chem. C*, **2008**, *112*, 18849-18859.

39) S. K. Dondapati, T. K. Sau, C. Hrelescu, T. A. Klar, F. D. Stefani and J. Feldmann, *ACS nano*, **2010**, *4*, 6318-6322.

40) J. Henzie, J. E. Barton, C. L. Stender and T. W. Odom, *Accounts. Chem. Res.*, **2006**, *39*, 249-257.

41) J. Aizpurua, G. W. Bryant, L. J. Richter, F. J. G. de Abajo, B. K. Kelley and T. Mallouk, *Phys. Rev. B*, **2005**, *71,* 235420.

42) A. M. Funston, C. Novo, T. J. Davis and P. Mulvaney, *Nano. Lett.*, **2009**, *9*, 1651-1658.

43) S. L. Smitha, K. G. Gopchandran, T. R. Ravindran and V. S. Prasad, *Nanotechnology* **2011**, *22,* 265705.

44) K. Yang, F. J. Zhang, H. Tang, C. Zhao, Y. A. Cao, X. Q. Lv, D. Chen and Y. D. Li, *Int. J. Nanomed.*, **2011**, *6*, 1739-1745.

45) S. A. Sarkis, B. H. Abdullah, B. A. A. Majeed and N. G. Talabani, *Head Neck Oncol.*, **2010**, *2*. doi: 10.1186/1758-3284-**2**-13

46) V. F. Bernardes, F. O. Gleber-Netto, S. F. Sousa, T. A. Silva and M. C. F. Aguiar, *J. Exp. Clin. Canc. Res.*, **2010**, *29*. doi: 10.1186/1756-9966-29-40

View Article Online
DOI: 10.1039/C3RA46208K

Table of Contents Entry

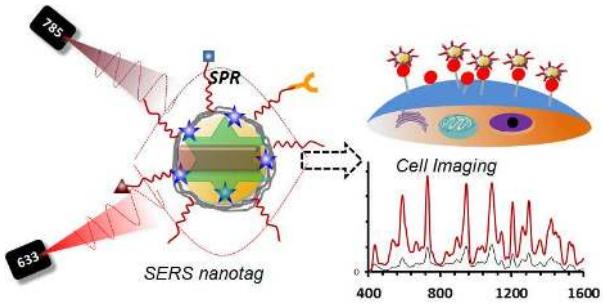

A systematic study on the influence of SERS signals enhancement leads to develop ultrasensitive nanotags for cancer cell imaging.